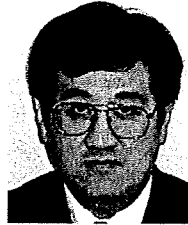


- [54] T. E. Lohmeier, A. M. Barrett, and E. D. Irwin, "Prolonged activation of the baroreflex: A viable approach for the treatment of hypertension?," *Curr. Hypertens. Rep.*, vol. 7, no. 3, pp. 193–198, Jun. 2005.
- [55] T. E. Lohmeier, D. A. Hildebrandt, T. M. Dwyer, A. M. Barrett, E. D. Irwin, M. A. Rossing, and R. S. Kieval, "Renal denervation does not abolish sustained baroreflex-mediated reductions in arterial pressure," *Hypertension*, vol. 49, no. 2, pp. 373–379, Feb. 2007.
- [56] T. E. Lohmeier, T. M. Dwyer, E. D. Irwin, M. A. Rossing, and R. S. Kieval, "Prolonged activation of the baroreflex abolishes obesity-induced hypertension," *Hypertension*, vol. 49, no. 6, pp. 1307–1314, Jun. 2007.
- [57] T. E. Lohmeier, D. A. Hildebrandt, T. M. Dwyer, R. Ilescu, E. D. Irwin, A. W. Cates, and M. A. Rossing, "Prolonged activation of the baroreflex decreases arterial pressure even during chronic adrenergic blockade," *Hypertension*, vol. 53, no. 5, pp. 833–838, May 2009.
- [58] T. N. Thrasher, "Unloading arterial baroreceptors causes neurogenic hypertension," *Amer. J. Physiol.*, vol. 282, no. 4, pp. R1044–R1053, Apr. 2002.
- [59] T. N. Thrasher, "Baroreceptors and the long-term control of blood pressure," *Exp. Physiol.*, vol. 89, no. 4, pp. 331–335, Jul. 2004.
- [60] C. J. Dickinson, "Re: Baroreceptors and the long-term control of blood pressure," *Exp. Physiol.*, vol. 89, no. 4, pp. 335–337, Jul. 2004.
- [61] P. Sleight, "Arterial baroreflexes can determine long-term blood pressure. Baroreceptors and hypertension: Time for a re-think?," *Exp. Physiol.*, vol. 89, no. 4, pp. 337–341, Jul. 2004.
- [62] T. N. Thrasher, "Effects of chronic baroreceptor unloading on blood pressure in the dog," *Amer. J. Physiol.*, vol. 288, no. 4, pp. R863–R871, Apr. 2005.
- [63] T. N. Thrasher, "Baroreceptors, baroreceptor unloading, and the long-term control of blood pressure," *Amer. J. Physiol.*, vol. 288, no. 4, pp. R819–R827, Apr. 2005.
- [64] T. N. Thrasher, "Arterial baroreceptor input contributes to long-term control of blood pressure," *Curr. Hypertens. Rep.*, vol. 8, no. 3, pp. 249–254, Jun. 2006.
- [65] P. A. Munch, M. C. Andresen, and A. M. Brown, "Rapid resetting of aortic baroreceptors in vitro," *Amer. J. Physiol.*, vol. 244, no. 5, pp. H672–H680, May 1983.
- [66] H. R. Warner, "The frequency-dependent nature of blood pressure regulation by the carotid sinus studied with an electric analog," *Circ. Res.*, vol. 6, no. 1, pp. 35–40, Jan. 1958.
- [67] D. Michikami, A. Kamiya, T. Kawada, M. Inagaki, T. Shishido, K. Yamamoto, H. Ariumi, S. Iwase, J. Sugeno, K. Sunagawa, and M. Sugimachi, "Short-term electroacupuncture at Zusanli resets the arterial baroreflex neural arc toward lower sympathetic nerve activity," *Amer. J. Physiol.*, vol. 291, no. 1, pp. H318–H326, Jul. 2006.
- [68] M. Sugimachi, T. Kawada, H. Yamamoto, A. Kamiya, T. Miyamoto, and K. Sunagawa, "Modification of autonomic balance by electrical acupuncture does not affect baroreflex dynamic characteristics," in *Conf. Proc. IEEE Eng. Med. Biol. Soc.*, 2008, vol. 2008, pp. 1981–1984.
- [69] T. Kawada, S. Shimizu, H. Yamamoto, T. Shishido, A. Kamiya, T. Miyamoto, K. Sunagawa, and M. Sugimachi, "Servo-controlled hind-limb electrical stimulation for short-term arterial pressure control," *Circ. J.*, vol. 73, no. 5, pp. 851–859, May 2009.
- [70] H. Yamamoto, T. Kawada, A. Kamiya, T. Kita, and M. Sugimachi, "Electroacupuncture changes the relationship between cardiac and renal sympathetic nerve activities in anesthetized cats," *Auton. Neurosci.*, vol. 144, no. 1–2, pp. 43–49, Dec. 2008.
- [71] Y. Yanagiya, T. Sato, T. Kawada, M. Inagaki, T. Tatewaki, C. Zheng, A. Kamiya, H. Takaki, M. Sugimachi, and K. Sunagawa, "Bionic epidural stimulation restores arterial pressure regulation during orthostasis," *J. Appl. Physiol.*, vol. 97, no. 3, pp. 984–990, Sep. 2004.
- [72] F. Yamasaki, T. Ushida, T. Yokoyama, M. Ando, K. Yamashita, and T. Sato, "Artificial baroreflex: Clinical application of a bionic baroreflex system," *Circulation*, vol. 113, no. 5, pp. 634–639, Feb. 2006.
- [73] K. Yamamoto, T. Kawada, A. Kamiya, H. Takaki, T. Shishido, K. Sunagawa, and M. Sugimachi, "Muscle mechanoreflex augments arterial baroreflex-mediated dynamic sympathetic response to carotid sinus pressure," *Amer. J. Physiol.*, vol. 295, no. 3, pp. H1081–H1089, Sep. 2008.
- [74] K. Yamamoto, T. Kawada, A. Kamiya, H. Takaki, M. Sugimachi, and K. Sunagawa, "Static interaction between muscle mechanoreflex and arterial baroreflex in determining efferent sympathetic nerve activity," *Amer. J. Physiol.*, vol. 289, no. 4, pp. H1604–H1609, Oct. 2005.
- [75] K. Yamamoto, T. Kawada, A. Kamiya, H. Takaki, T. Miyamoto, M. Sugimachi, and K. Sunagawa, "Muscle mechanoreflex induces the pressor response by resetting the arterial baroreflex neural arc," *Amer. J. Physiol.*, vol. 286, no. 4, pp. H1382–H1388, Apr. 2004.
- [76] M. Yoshida, Y. Murayama, A. Chishaki, and K. Sunagawa, "Noninvasive transcutaneous bionic baroreflex system prevents severe orthostatic hypotension in patients with spinal cord injury," in *Conf. Proc. IEEE Eng. Med. Biol. Soc.*, 2008, vol. 2008, pp. 1985–1987.
- [77] J. N. Townsend and W. A. Littler, "Cardiac vagal activity: A target for intervention in heart disease," *Lancet*, vol. 345, no. 8955, pp. 937–938, Apr. 1995.
- [78] M. Li, C. Zheng, T. Sato, T. Kawada, M. Sugimachi, and K. Sunagawa, "Vagal nerve stimulation markedly improves long-term survival after chronic heart failure in rats," *Circulation*, vol. 109, no. 1, pp. 120–124, Jan. 2004.
- [79] C. Zheng, M. Li, M. Inagaki, T. Kawada, K. Sunagawa, and M. Sugimachi, "Vagal stimulation markedly suppresses arrhythmias in conscious rats with chronic heart failure after myocardial infarction," in *Conf. Proc. IEEE Eng. Med. Biol. Soc.*, 2005, vol. 7, pp. 7072–7075, 1.
- [80] M. Li, C. Zheng, M. Inagaki, T. Kawada, K. Sunagawa, and M. Sugimachi, "Chronic vagal stimulation decreased vasopressin secretion and sodium ingestion in heart failure rats after myocardial infarction," in *Conf. Proc. IEEE Eng. Med. Biol. Soc.*, 2005, vol. 4, pp. 3962–3965.
- [81] T. Kawada, T. Yamazaki, T. Akiyama, M. Li, H. Ariumi, H. Mori, K. Sunagawa, and M. Sugimachi, "Vagal stimulation suppresses ischemia-induced myocardial interstitial norepinephrine release," *Life Sci.*, vol. 78, no. 8, pp. 882–887, Jan. 2006.
- [82] T. Kawada, T. Yamazaki, T. Akiyama, H. Kitagawa, S. Shimizu, M. Mizuno, M. Li, and M. Sugimachi, "Vagal stimulation suppresses ischemia-induced myocardial interstitial myoglobin release," *Life Sci.*, vol. 83, no. 13–14, pp. 490–495, Sep. 2008.
- [83] K. Uemura, M. Li, T. Tsutsumi, T. Yamazaki, T. Kawada, A. Kamiya, M. Inagaki, K. Sunagawa, and M. Sugimachi, "Efferent vagal nerve stimulation induces tissue inhibitor of metalloproteinase-1 in myocardial ischemia-reperfusion injury in rabbit," *Amer. J. Physiol.*, vol. 293, no. 4, pp. H2254–H2261, Oct. 2007.
- [84] L. V. Borovikova, S. Ivanova, M. Zhang, H. Yang, G. I. Botchkina, L. R. Watkins, H. Wang, N. Abumrad, J. W. Eaton, and K. J. Tracey, "Vagus nerve stimulation attenuates the systemic inflammatory response to endotoxin," *Nature*, vol. 405, no. 6785, pp. 458–462, May 2000.
- [85] K. J. Tracey, "The inflammatory reflex," *Nature*, vol. 420, no. 6917, pp. 853–859, Dec. 2002.
- [86] H. Wang, M. Yu, M. Ochani, C. A. Amella, M. Tanovic, S. Susarla, J. H. Li, H. Wang, H. Yang, L. Ulloa, Y. Al-Abed, C. J. Czura, and K. J. Tracey, "Nicotinic acetylcholine receptor $\alpha 7$ subunit is an essential regulator of inflammation," *Nature*, vol. 421, no. 6821, pp. 384–388, Jan. 2003.
- [87] K. J. Tracey and H. S. Warren, "Human genetics: An inflammatory issue," *Nature*, vol. 429, no. 6987, pp. 35–37, May 2004.
- [88] J. Springer, D. O. Okonko, and S. D. Anker, "Vagal nerve stimulation in chronic heart failure: An antiinflammatory intervention?," *Circulation*, vol. 110, no. 4, p. e34, Jul. 2004.
- [89] S. Guarini, D. Altavilla, M. M. Cainazzo, D. Giuliani, A. Bigiani, H. Marini, G. Squadrito, L. Minutoli, A. Bertolini, R. Marini, E. B. Adamo, F. S. Venuti, and F. Squadrito, "Efferent vagal fibre stimulation blunts nuclear factor-kappaB activation and protects against hypovolemic hemorrhagic shock," *Circulation*, vol. 107, no. 8, pp. 1189–1194, Mar. 2003.
- [90] G. M. De Ferrari, A. Sanzo, H. J. G. M. Crijns, R. Dennert, G. Milasinovic, S. Raspopovic, M. Borggrefe, C. Wolpert, J. Kuschyk, A. Schoene, H. Klein, J. Smid, A. Gavazzi, M. Zabel, and P. J. Schwartz, *Chronic Vagus Nerve Stimulation: A New Treatment Modality for Congestive Heart Failure*. Orlando, FL: American College of Cardiology, 2009.
- [91] I. H. Zucker, J. F. Hackley, K. G. Cornish, B. A. Hiser, N. R. Anderson, R. Kieval, E. D. Irwin, D. J. Serdar, J. D. Peuler, and M. A. Rossing, "Chronic baroreceptor activation enhances survival in dogs with pacing-induced heart failure," *Hypertension*, vol. 50, no. 5, pp. 904–910, Nov. 2007.
- [92] G. I. Voss, P. G. Katona, and H. J. Chizeck, "Adaptive multivariable drug delivery: Control of arterial pressure and cardiac output in anesthetized dogs," *IEEE Trans. Biomed. Eng.*, vol. BE-34, pp. 617–623, Aug. 1987.

- [93] C. Yu, P. J. Roy, H. Kaufman, and B. W. Bequette, "Multiple-model adaptive predictive control of mean arterial pressure and cardiac output," *IEEE Trans. Biomed. Eng.*, vol. 39, pp. 765–778, Aug. 1992.
- [94] K. Uemura, M. Sugimachi, T. Kawada, A. Kamiya, Y. Jin, K. Kashihara, and K. Sunagawa, "A novel framework of circulatory equilibrium," *Amer. J. Physiol.*, vol. 286, no. 6, pp. H2376–H2385, Jun. 2004.
- [95] A. C. Guyton, A. W. Lindsey, B. Abernathy, and T. Richardson, "Venous return at various right atrial pressures and the normal venous return curves," *Amer. J. Physiol.*, vol. 189, no. 3, pp. 609–615, Jun. 1957.
- [96] K. Sagawa, L. Maughan, H. Suga, and K. Sunagawa, *Cardiac Contraction and the Pressure-Volume Relationship*. New York: Oxford Univ. Press, 1988, ch. 5, pp. 232–298.
- [97] K. Uemura, T. Kawada, A. Kamiya, T. Aiba, I. Hidaka, K. Sunagawa, and M. Sugimachi, "Prediction of circulatory equilibrium in response to changes in stressed blood volume," *Amer. J. Physiol.*, vol. 289, no. 1, pp. H301–H307, Jul. 2005.
- [98] K. Uemura, A. Kamiya, I. Hidaka, T. Kawada, S. Shimizu, T. Shishido, M. Yoshizawa, M. Sugimachi, and K. Sunagawa, "Automated drug delivery system to control systemic arterial pressure, cardiac output, and left heart filling pressure in acute decompensated heart failure," *J. Appl. Physiol.*, vol. 100, no. 4, pp. 1278–1286, Apr. 2006.
- [99] K. Uemura, K. Sunagawa, and M. Sugimachi, "Computationally managed bradycardia improved cardiac energetics while restoring normal hemodynamics in heart failure," *Ann. Biomed. Eng.*, vol. 37, no. 1, pp. 82–93, Jan. 2009.
- [100] K. Hayashida, K. Sunagawa, M. Noma, M. Sugimachi, H. Ando, and M. Nakamura, "Mechanical matching of the left ventricle with the arterial system in exercising dogs," *Circ. Res.*, vol. 71, no. 3, pp. 481–489, Sep. 1992.
- [101] M. Sugimachi, K. Todaka, K. Sunagawa, and M. Nakamura, "Optimal afterload for the heart vs. optimal heart for the afterload," *Front. Med. Biol. Eng.*, vol. 2, no. 3, pp. 217–221, 1990.



Masaru Sugimachi (A'98–M'06) received the M.D. degree and the Ph.D. degree in biomedical engineering from Kyushu University, Fukuoka, Japan, in 1984 and 1992, respectively.

He is the Director of the Department of Cardiovascular Dynamics, National Cardiovascular Center Research Institute, Osaka, Japan, which he joined in 1992. There, he integrated the research team for the clinical application of bionic cardiology. Since 2004, he has chaired the department. He has published more than 160 original papers in cardiac mechanics, cardiovascular regulation, modeling of biological systems, and bionic medicine. He has been a Principal Investigator of two national research projects (implantable cardiac autonomic neuroregulators, next-generation ICDs) and is currently a Principal Investigator of two other projects (distributed micropacemakers and intensive cardiac care autopilot system).



Kenji Sunagawa (M'95–SM'06) received the M.D. degree and the Ph.D. degree in biomedical engineering from Kyushu University, Fukuoka, Japan, in 1974 and 1985, respectively.

He is Chairman of and a Professor in the Department of Cardiovascular Medicine, Graduate School of Medical Sciences, Kyushu University. He has been a member of the Administrative Committee of the Japanese Society of Medical Electronics and Biological Engineering. In 1978, he joined the Department of Biomedical Engineering, The Johns Hopkins Medical School, where he established the concept of ventricular-arterial coupling. The coupling concept has been adopted for many textbooks of cardiology and cardiac physiology worldwide. From 1992 to 2004, he chaired the Department of Cardiovascular Dynamics, the National Cardiovascular Center, Osaka, Japan, and developed the basis of bionic cardiology.

An Analysis of Interference Mitigation Capability of Low Duty-Cycle UWB Communications in the Presence of Wideband OFDM System

Keisuke Sodeyama · Koji Ishibashi · Ryuji Kohno

© Springer Science+Business Media, LLC. 2009

Abstract Low duty-cycle (LDC) algorithm is interference mitigation technique, which can reduce the average interference to the existing radio systems by lowering pulse repetition interval or pulse occupation time. In this paper, the coexistence environment between low data rate ultra wideband (UWB) communication system such as wireless sensor network and the existing wideband system using orthogonal frequency division multiplexing (OFDM) such as 4th generation mobile cellular system (4G), worldwide interoperability for microwave access (WiMAX), and field pickup unit (FPU) is considered. In order to analyze the interference mitigation capability of LDC algorithm with impulse based UWB (LDC-UWB) system, the frame error rate (FER) of wideband OFDM system is examined for two types of LDC-UWB system: the signal with random polarity such as binary pole signals and without random polarity such as mono pole signals. We present that LDC algorithm is an efficient interference mitigation technique for low data rate UWB communication via computer simulations regardless of definitions of transmitted energy of UWB communication system, and also that the signal with random polarity is suitable for LDC-UWB system to mitigate interference to the other radio systems. We further investigate the adequate duty-cycle of LDC-UWB system for each definition of transmitted power of UWB communication.

Keywords Low duty-cycle · LDC-UWB · Interference mitigation technique · Wideband OFDM system

K. Sodeyama (✉) · R. Kohno
Division of Physics, Electrical and Computer Engineering, Graduate School of Engineering,
Yokohama National University, 79-5, Tokiwadai, Hodogaya-ku, Yokohama,
Kanagawa 240-8501, Japan
e-mail: sodeyama@kohnolab.dnj.ynu.ac.jp

K. Ishibashi
Department of Electrical and Electronic Engineering, Faculty of Engineering, Shizuoka University,
3-5-1, Johoku, Naka-ku, Hamamatsu, Shizuoka 432-8561, Japan

1 Introduction

As increasing wireless applications and the quantity of digital information, more efficient digital communications are highly required. Thus, some new technologies such as ultra wideband (UWB) communication systems have been proposed for short-range wireless applications [1,2]. UWB communication has also gained much attention as coexistence with other radio systems because of its low power spectrum density equivalent to noise level. The potential applications of UWB communication include high data rate wireless personal area network (WPAN) which can achieve more than 100 Mbps over short distance and wireless sensor networks such as IEEE 802.15.4a providing low data rate UWB communication over medium range combined with precise ranging and positioning capabilities. Thus, UWB communication is a promised technology to apply various application. While wireless local area network (WLAN) and Bluetooth coexist each other and also with the other unlicensed systems in the industry, science, and medical (ISM) band which is opened for some applications in Japan, UWB communication coexist with licensed system such as worldwide interoperability for microwave access (WiMAX), 4th generation mobile cellular systems (4G), and field pickup unit (FPU). Therefore, UWB communication may inherently degrade the performance of the existing other radio systems since the radio band of the UWB communication systems overlaps that of the other radio systems such as WiMAX, 4G, and FPU. The technical conditions on the usage of UWB communication system were set up by the Ministry of Internal Affairs and Communications on March 2006, in Japan [3] and it is imperative for UWB communications to equip the interference mitigation techniques, *detect and avoid* (DAA) [4–15] and *low duty-cycle* (LDC) [16–20].

In general, DAA technique aims to mainly at high data rate UWB communication such as WPAN. The device with DAA can detect the signals from other radio systems and avoid interference to them. Although UWB communication systems with DAA technique are allowed to transmit with power level of -41.25 dBm/MHz, those without DAA technique must limit their emission level by -70 dBm/MHz which is lower than the noise level. Namely, unless interference mitigation techniques are adopted, the emission level of UWB signals is 30 dB lower than FCC UWB indoor environment spectral mask to meet the current regulation in Japan. High data rate UWB communication with DAA techniques have been studied in the literature [4–8]. DAA techniques are divided into three types: frequency domain DAA [9–12], time domain DAA [13,14] and space domain DAA [15]. For frequency domain DAA techniques the UWB devices detect the radio frequency band of the other existing radio system and avoid interference to these system by using frequency hopping, transmit power control, frequency filter and so on [9–12]. UWB communication system with time domain DAA techniques, which are very similar to carrier sense multiple access with collision avoidance (CSMA/CA) sense the existing radio systems before establishing data communication link [13,14]. Space domain DAA technique have been proposed that UWB communication systems can mitigate the interference to the existing radio systems by using spatial beam-forming of array antennas [15].

On the other hand, LDC algorithm mainly aims to low data rate UWB communications such as IEEE 802.15.4a [16]. IEEE 802.15.4a standard for low data rate sensor networks is designed for long battery life, low cost, and low latency rather than maximizing the data rate. Thus, DAA technique may not be suited for low data rate UWB communication because of their strict constraints on energy consumption and costs. Therefore, LDC algorithm can be an attractive candidate for interference mitigation in low data rate UWB communications.

The aim of LDC algorithm is to reduce the average interference to the existing radio systems by lowering pulse repetition interval or pulse occupation time. The features of LDC

algorithm imposes low data rate but achieve low energy consumption since the pulse repetition interval is extended. Originally, LDC algorithm has been proposed to reduce energy consumption [17]. Moreover, in UWB ad-hoc network, LDC algorithm has been studied to improve the near/far power disparities or pulse-on-pulse interference of multiple access [18, 19]. Furthermore, in low power low rate UWB communication, LDC algorithm has been studied to improve the protocol design of medium access control (MAC) layer [20].

However, the design of the duty-cycle of impulse-based UWB communication system with LDC algorithm (LDC-UWB) has not been presented. In addition, despite all the benefits inherent to LDC algorithm, UWB communication systems still interfere with the existing other radio systems. In this paper, we focus on the coexistence environment between LDC-UWB system and wideband system based on orthogonal frequency division multiplexing (OFDM) such as 4G, WiMAX, and FPU. This paper analyzes the performance of UWB system with LDC algorithm as the interference mitigation technique in the presence of coexistence environment. In order to analyze the interference mitigation capability of LDC-UWB, the performance of wideband OFDM systems based on the frame error rate (FER) over the coexistence environment is presented via computer simulations of C language. Moreover, two types of LDC-UWB signal interference are considered: the signal with random polarity such as binary pole signals and without random polarity such as mono pole signals. We present that LDC algorithm is an efficient interference mitigation technique for low data rate UWB communication. In addition, the definition of UWB transmission power has been approached in two different manners: fixed power per pulse and fixed power per unit of time. The question that may arise at this point is how to design the duty-cycle of LDC-UWB system by each definition of UWB transmission power. Therefore, we further investigate the adequate duty-cycle of LDC-UWB system for each definition.

The rest of this paper is organized as follows. Section 2 describes the LDC-UWB system model considered throughout this paper. The wideband OFDM system model is presented in Sect. 3. The simulation results are presented in Sect. 4. Finally, the conclusions are drawn in Sect. 5.

2 LDC-UWB System Model

The major parameters of UWB communication systems are given in Table 1. In this paper, low data rate UWB communication system is considered such as wireless sensor network, and thus, its data rate is below 1 MHz bits per second (bps). Also, the pulse repetition frequency (PRF) is given as 3.9 or 15.6 MHz, which is compliant with IEEE 802.15.4a. Also, PRF is defined as the number of the pulse in one frame of the transmit slot of LDC-UWB device.

Moreover, two types of LDC-UWB signal interference are considered: with random polarity such as binary pole signals and without random polarity such as mono pole signals. The reason for the later is the significant simplicity of the circuit design when using the signal without random polarity. We also consider two definitions of LDC-UWB transmission power: fixed power per pulse and fixed power per unit of time since these definitions have been discussed at the mutual interference between pulse-based UWB system and other radio system.

2.1 Specifications of LDC-UWB System

In this protocol, every UWB communication devices only wake up for short time to communicate with each other and timing schedule for communication is not available at each device.

Table 1 Major parameters of LDC-UWB systems

Type of UWB system	Impulse based UWB
Center frequency: f_c	4.0 GHz
Bandwidth	2 GHz
Data rate	> 1 Mbps
Pulse repetition frequency (PRF)	3.9 MHz, 15.6 MHz
Pulse width	0.5 ns
Duty-cycle: DC	0.1, 0.5, 1, 10, 50, 100%
Tx (or Rx) slot length	1–1,001 ms
Sleep period after Tx (or Rx)	1,000–0 ms
Frame length of LDC-UWB system	2,002 ms

Thus, in order to establish a communication link, access controller (AC) is introduced. The wireless network based on LDC protocol must have one AC device, which may be allowed relatively high power consumption and high duty-cycle (HDC) compared with those of non-AC devices. AC can receive messages from all UWB devices belonging to its own network besides having AC has the timing schedule of every UWB devices. Note that this protocol is suitable for indoor applications since AC device should be connected to the power supply because of its high power consumption and high duty-cycle. Figure 1 illustrates an example of the LDC protocol with UWB devices A and B, where, the duty-cycle is about 0.1% with both UWB devices transmit (Tx) and receive (Rx) time slot length of 1 ms. AC has 2,002 ms receive time slot and the duty-cycle of LDC-UWB system is defined as

$$DC = \frac{2T_s}{T_f}, \quad (1)$$

where DC is the duty-cycle of LDC-UWB, T_s is the Tx + Rx slot length, T_f is the frame length of LDC-UWB (T_f is fixed 2,002 ms). As example, duty-cycle 0.1% is defined that Tx and Rx of UWB communication devices are 1 ms, respectively, and total sleep period per frame is 2,000 ms, duty-cycle 50% is defined that Tx and Rx are 500 ms and total sleep period per frame is 1,002 ms.

The maximal number of interference pulse N_p is defined as

$$N_p = L_{Tx} \times DC \times f_{PRF}, \quad (2)$$

where L_{Tx} is the transmission frame length of LDC-UWB, DC is the duty-cycle of LDC-UWB system and f_{PRF} is the PRF of LDC-UWB system.

Device A keeps on sending a communication request (Comm. Req.) message to AC including its own timing schedule and a request to communicate with device B until the Ack message received from AC. Simultaneously, device B keeps on sending a Query message until Replay message from AC device is received as illustrated in Fig. 1, where Replay message includes the timing schedule of device A and its request to communicate with device B. Then, device B adjusts its own timing schedule to that of device A and device B sends a Ready message to device A directly. Then, a communication link between devices A and B is established.

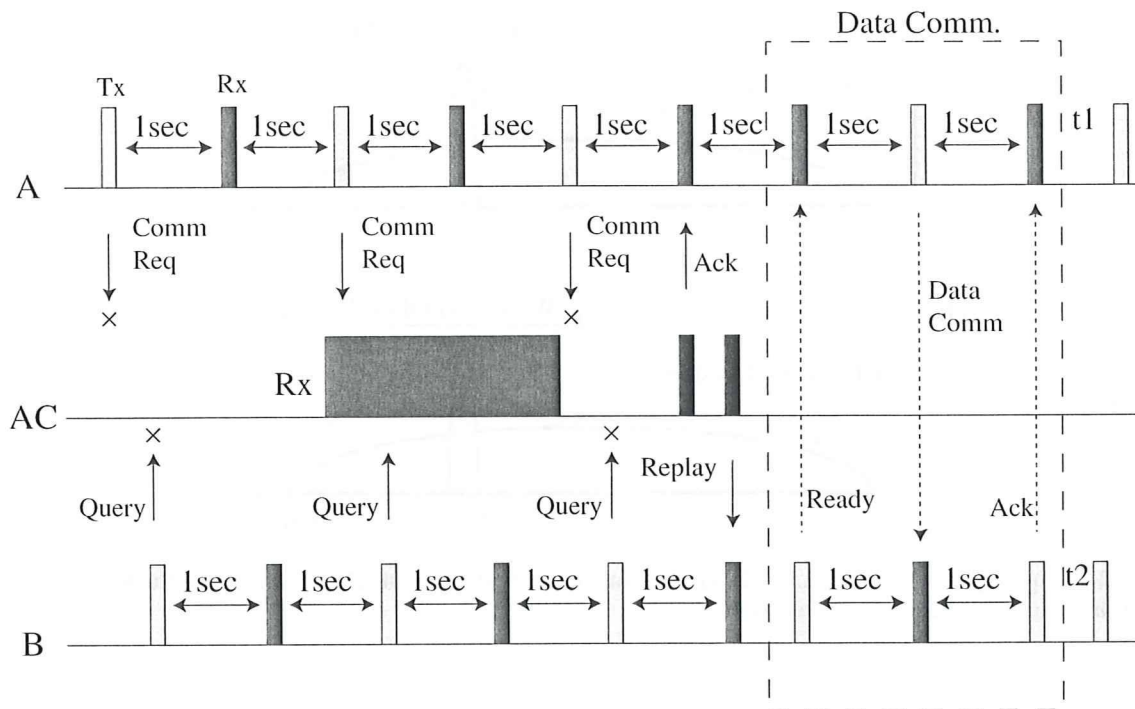


Fig. 1 an example of the LDC protocol with UWB communication devices A and B, where the duty-cycle is about 0.1%

2.2 Modified Equivalent Baseband UWB System

In this paper, UWB signal interference is modeled a modified equivalent baseband system [21]. UWB communication is permitted in Japan at the radio frequency from 3.4 to 4.8 GHz and from 7.25 to 10.25 GHz. At these frequencies, computer simulation are extremes time consuming owing to the high sampling frequency. Therefore, the simulation model implemented a modified equivalent baseband system in order to speed up the simulation. Figure 2 illustrates the spectral relation between the culprit LDC-UWB system and the wideband OFDM system, whose center frequencies are f_c and f_v , respectively, in the radio frequency (RF) domain. The wideband OFDM system is shifted from f_v to $f_v - f_c$ in order to tune the center frequency to specific frequency of the UWB signal in the modified equivalent baseband domain.

3 Wideband OFDM System Model

Wideband OFDM systems are considered among the most appropriate schemes for future high data rate communications systems due to their effective bandwidth utilization and the simplicity of the equalization strategies needed to compensate the channel frequency selective fading. The OFDM technique has been adopted in several standards, e.g., digital audio broadcasting (DAB), digital video broadcasting (DVB), multimedia mobile access communications (MMAC) and WLAN. It also has been proposed for cable TV, broadband radio access networks, multi-user communications via satellite link, WiMAX, 4G and FPU.

In this paper, we focus on the coexistence environment of UWB communication systems and wideband OFDM systems such as 4G and WiMAX. The basic idea of OFDM is to divide the available spectrum into several sub-channels (sub-carriers). By making all sub-channels

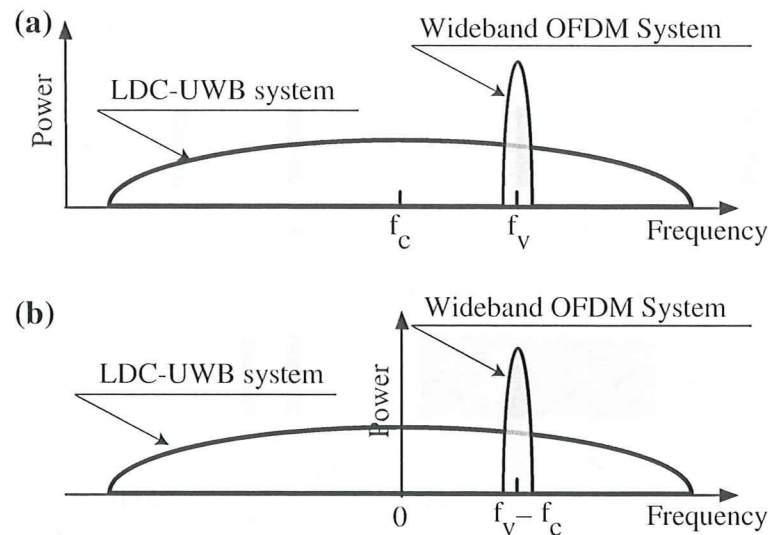


Fig. 2 Frequency spectra of the LDC-UWB system and the wideband OFDM system in: (a) the RF domain and (b) the modified equivalent baseband domain

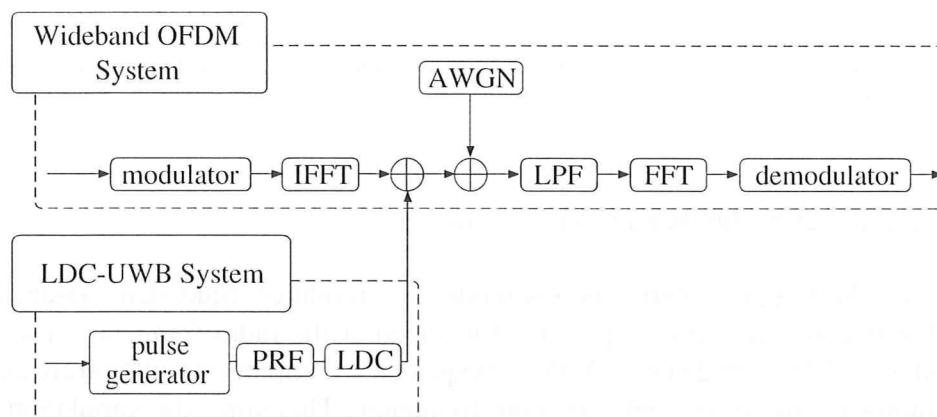


Fig. 3 The block diagram of the wideband OFDM system

narrower than the coherence bandwidth of the radio channels, they experience almost flat fading, simplifying the equalization process (one tap equalizer). In order to obtain a high spectral efficiency the sub-channels are overlapping, still keeping the orthogonality of their sub-carriers. This orthogonality is completely maintained, even when the signal passes through a time dispersive channel by introducing a cyclic prefix (the last part of the OFDM symbol is copied in front of the transmitted symbol). This of course introduces a loss in signal-to-noise ratio (SNR), but if the impulse response of channel is shorter than the cyclic prefix, then the inter-symbol interference (ISI) and inter-carrier interference (ICI) are completely removed at the output of the channel [22].

Figure 3 shows the block diagram of the wideband OFDM system. Major parameters of the wideband OFDM systems are listed in Table 2 (c.f., [23]). In this paper, the bandwidth of the wideband OFDM system is about 100 MHz and, thus, its data rate is 100 MHz bps. The equivalent baseband model is employed, therefore, the interference of the UWB signals is introduced by adding the UWB signal to the transmitted OFDM signal (see Fig. 3). After that, the received signals are passed through the low pass filter (LPF) of the wideband OFDM system.

Table 2 Major parameters of the wideband OFDM systems

Bandwidth	101.5 MHz
Data rate objective	>100 Mbits/s
Number of sub-carriers: N_c	768
Sub-carrier spacing: F_s	131.8 kHz
OFDM symbol duration: T_s	7.585 μ s
Total OFDM symbols duration: T'_s	9.259 μ s
Number of OFDM symbols per frame: N_s	54
OFDM frame length: T_{fr}	500 μ s
Symbol mapping	QPSK

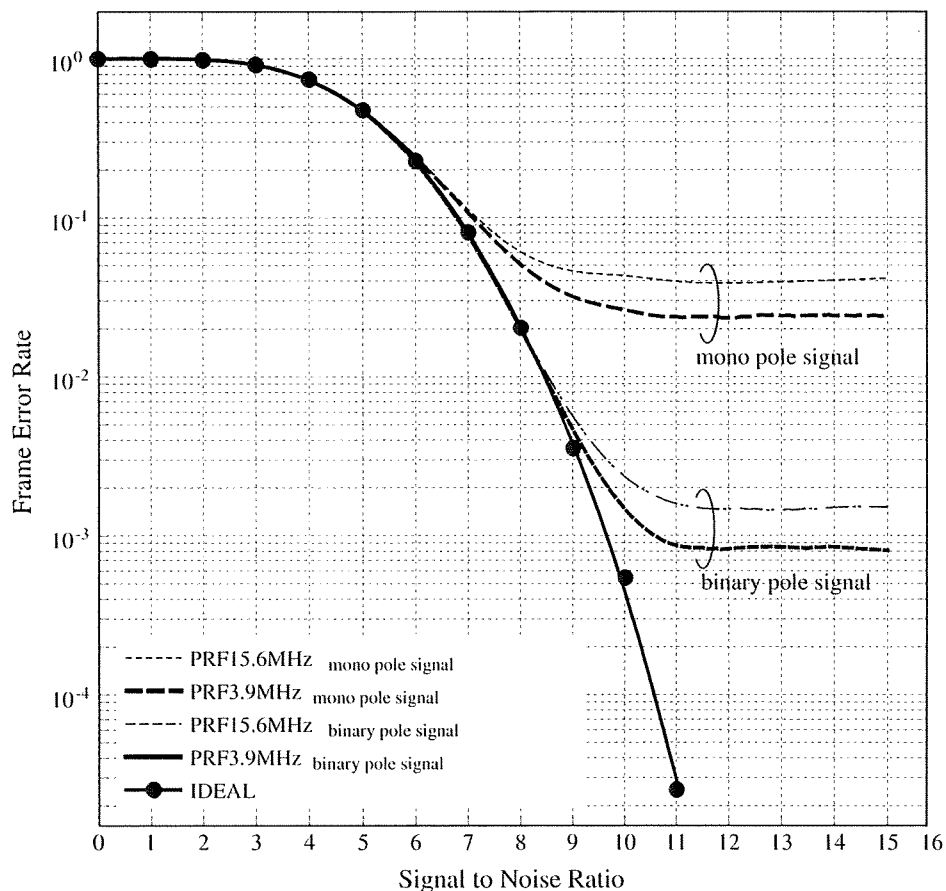


Fig. 4 The FER of the wideband OFDM system over AWGN channel with the interference by LDC-UWB system when SIR = 10dB and duty-cycle=0.1%. The definition of UWB transmission power is fixed power per pulse

4 Simulation Results

Although LDC protocol promises that the average interference to the wideband OFDM systems can be suppressed, LDC-UWB communication systems still interfere to wideband OFDM systems even with LDC protocol. Moreover, when UWB communication devices (or users) are increased, the interference to wideband OFDM system may be increased even applying lower duty-cycle.

First, the FER of the wideband OFDM systems over additive white Gaussian (AWGN) channel with the interference by the LDC-UWB system is analyzed. Figure 4 shows the FER

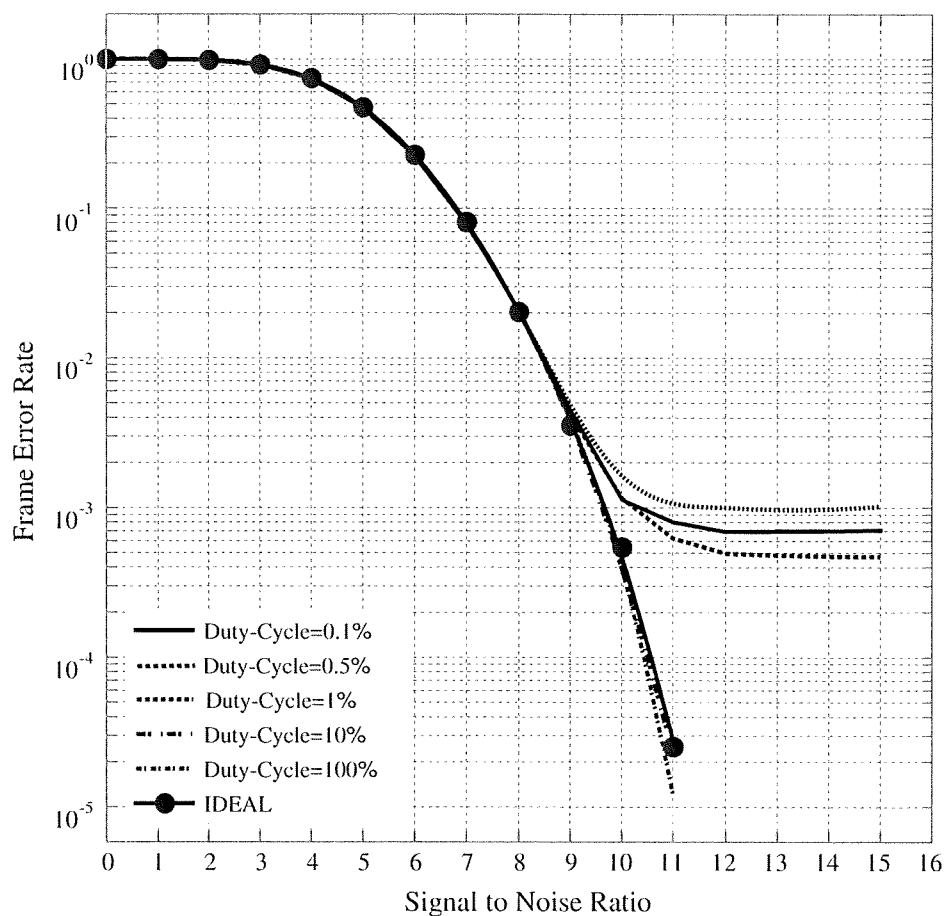


Fig. 5 The FER of the wideband OFDM systems over AWGN channel with the interference by LDC-UWB system when $SIR = 10$ dB and $PRF = 3.9$ MHz. The definition of UWB transmission power is fixed power per unit of time

of the wideband OFDM system with the interference by LDC-UWB system when signal to interference ratio (SIR) = 10 dB, duty-cycle is 0.1% and PRF is given as 3.9 or 15.9 MHz. Also, SIR is defined as the wideband OFDM system transmission power to LDC-UWB interference transmission power ratio. LDC-UWB transmission power is fixed power per pulse.

From Fig. 4, the FER of the wideband OFDM system with interference by binary pole signals is superior to the interference by mono pole signals. The reason for this to occur is that the LDC-UWB interference by mono pole signals amplifies the interference since the constant signal polarity adds to wideband OFDM system. Meanwhile, the interference by binary pole signal is reduced by the each random polarity of LDC-UWB signals. Therefore, LDC-UWB signal needs the random polarity such as binary pole signal. In other words, the binary pole signal is essential for LDC-UWB signal to reduce interference to wideband OFDM systems.

From another viewpoint, the FER of wideband OFDM systems are degraded by increasing PRF of LDC-UWB systems since the number of interference pulses are increased. Therefore, the PRF of LDC-UWB systems should be carefully chosen in consideration of the quality of performance required by wideband OFDM system and by each LDC-UWB application.

When the definition of LDC-UWB transmission power is fixed, the power per unit of time, the FER of wideband OFDM system with interference by LDC-UWB system with $SIR = 10$ dB, and $PRF = 3.9$ MHz is presented in Fig. 5. Figure 6 shows the performance when PRF is changed to 15.6 MHz.

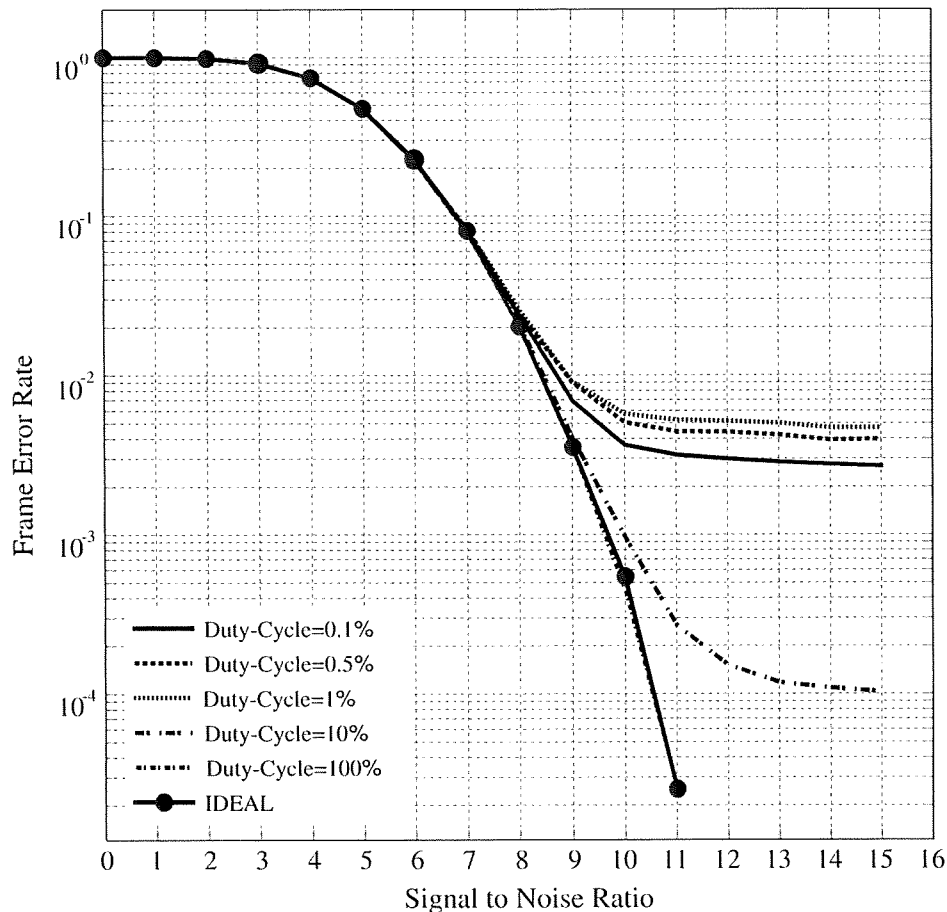


Fig. 6 The FER of the wideband OFDM systems over AWGN channel with the interference by LDC-UWB system when SIR = 10 dB and PRF = 15.6 MHz. The definition of UWB transmission power is fixed power per unit of time

From Figs. 5 and 6, when the definition of UWB transmission power is fixed power per unit of time, the FER of wideband OFDM systems is superior to that of fixed power per pulse since the transmission power of each pulses is reduced. Therefore, the collision probability considered, the interference of LDC-UWB system is improved as longer as duty-cycle. However, the communication area of LDC-UWB devices is narrowed since the signal power is reduced by increasing duty-cycle. Thus, a trade-off between the communication area of LDC-UWB devices and duty-cycle of LDC-UWB system can be found. Moreover, the FER of wideband OFDM systems are degraded by decreasing PRF of LDC-UWB systems since the power of each pulses are decreasing.

Secondly, the FER of wideband OFDM system over AWGN channel with the interference by LDC-UWB systems is presented when the duty-cycle of LDC-UWB system is changed. Here, SNR is fixed to 10 dB. The FER of the wideband OFDM systems with the interference by the LDC-UWB communication devices are shown in Fig. 7, where PRF = 3.9 MHz. Figure 8 shows the performance when PRF = 15.6 MHz. Here, the definition of LDC-UWB transmission power is fixed power the pulse.

From Figs. 7 and 8, the FER of wideband OFDM systems are degraded by increasing of the duty-cycle of LDC-UWB systems. LDC cannot suppress interference to wideband OFDM systems completely. However it can be mitigated moderately without additional complexity such as DAA. Thus, the duty-cycle of LDC-UWB should be chosen carefully in consideration of the quality of the service required by the wideband OFDM system in the physical layer.

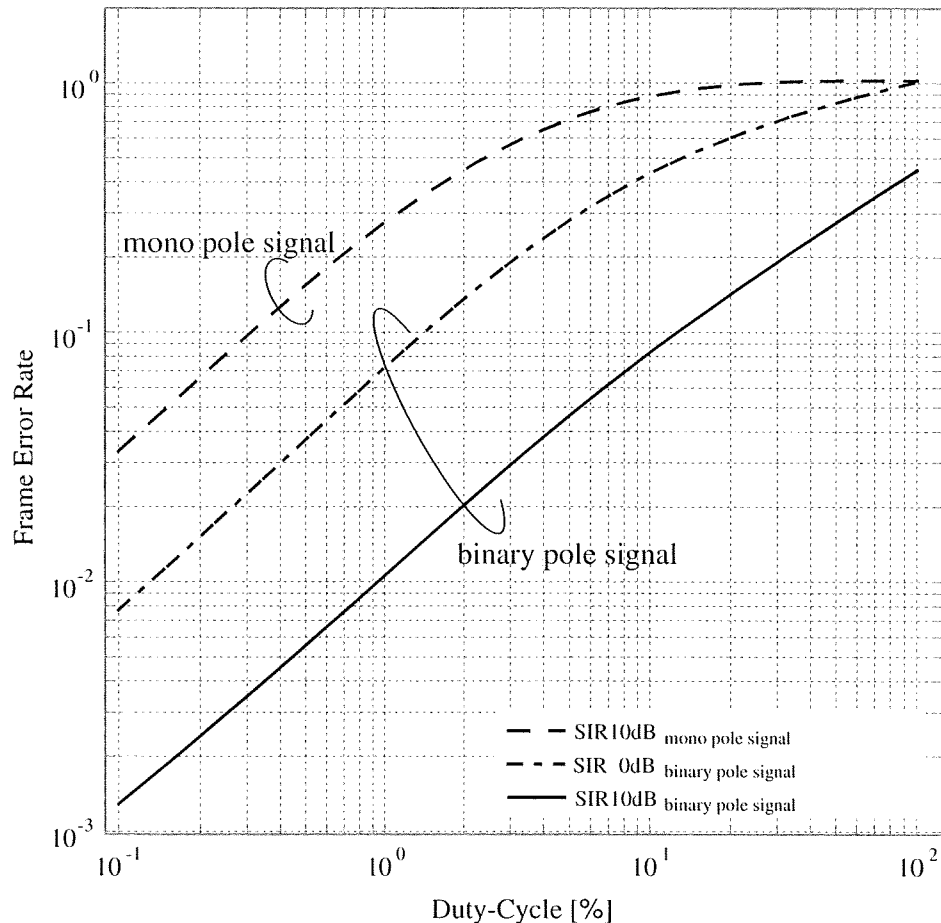


Fig. 7 The FER of the wideband OFDM system with the interference by the LDC-UWB communication devices, when SNR=10dB and the PRF=3.9MHz. The definition of UWB transmission power is fixed power per pulse

When the LDC-UWB signal power is fixed power per unit of time, the FER of wideband OFDM system with the interference by changing the duty-cycle of LDC-UWB system is presented. Here, SNR is fixed to 10dB. Figure 9 shows the FER of the wideband OFDM systems with the interference by LDC-UWB communication devices.

In Fig. 9, the FER of wideband OFDM system with interference by duty-cycle=100% is superior to that of duty-cycle=0.1%. For the reason that although the collision probability between wideband OFDM system and LDC-UWB system is increased, the pulse signal power becomes lower since the number of pulses is increased. However, when the duty-cycle of DC-UWB system is increased, simultaneously, the power consumption is also grown. Therefore, in IEEE 802.15.4a, such as wireless sensor network, using duty-cycle=100% is difficult. Therefore, the duty-cycle of LDC-UWB system should be set to distinctly low values of <math><0.1\%</math>.

From these results, the duty-cycle of LDC-UWB system should be chosen carefully in consideration of the requirements of the each LDC-UWB applications. When the LDC-UWB signal power is fixed power per pulse, the interference to wideband OFDM is mitigated with reducing duty-cycle of LDC-UWB system. Therefore, when the LDC-UWB signal power is fixed power per pulse, the duty-cycle of LDC-UWB should be chosen low values of 0.1% and using PRF=3.9 MHz is absolutely essential. Meanwhile, when the LDC-UWB signal power is fixed power per unit of time, the duty-cycle of LDC-UWB system is depended on both the collision probability between wideband OFDM system and LDC-UWB system

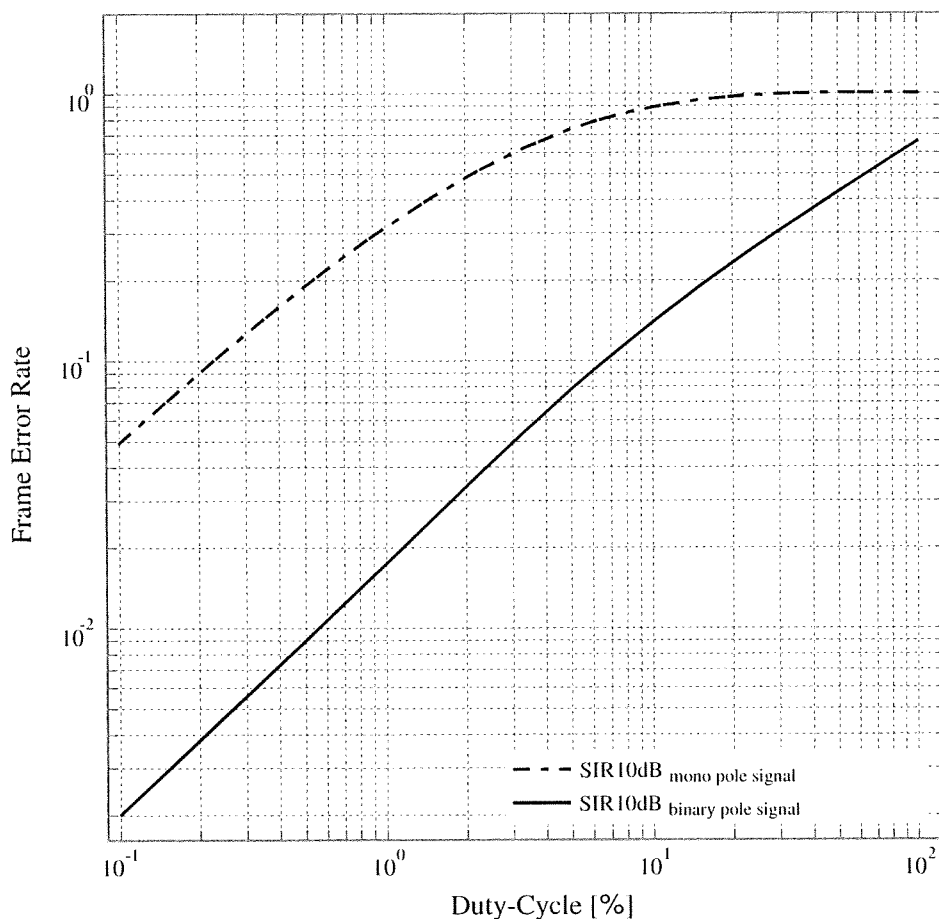


Fig. 8 The FER of the wideband OFDM system with the interference by the LDC-UWB communication devices, when SNR=10dB and the PRF=15.6MHz. The definition of UWB transmission power is fixed the power per the pulse

and the power of LDC-UWB pulse. In IEEE 802.15.4a such as wireless sensor network, using higher duty-cycle is difficult since the power consumption is also significantly high. Therefore, when the LDC-UWB signal power is fixed power per unit of time, the duty-cycle of LDC-UWB should be set to distinctly low values of $<0.1\%$ and using PRF=15.6MHz is absolutely essential. Thus, the design issues of PRF and duty-cycle are different with each definition of LDC-UWB transmission power.

5 Conclusions

In this paper, we have focused on the coexistence environment between LDC-UWB system and wideband OFDM system and have analyzed the interference mitigation capability of LDC-UWB system in the presence of wideband OFDM system. The performance of wideband OFDM system based on FER over the coexistence environment has been presented via computer simulations. The signal with random polarity such as binary pole signal has been necessary to mitigate the interference for wideband OFDM system. Moreover, by the definition of the UWB transmission power, the duty-cycle of LDC-UWB system has been needed to establish in consideration of the request of the each LDC-UWB application. Moreover, we have presented the design issues of PRF and duty-cycle are different with each definition of LDC-UWB transmission power.

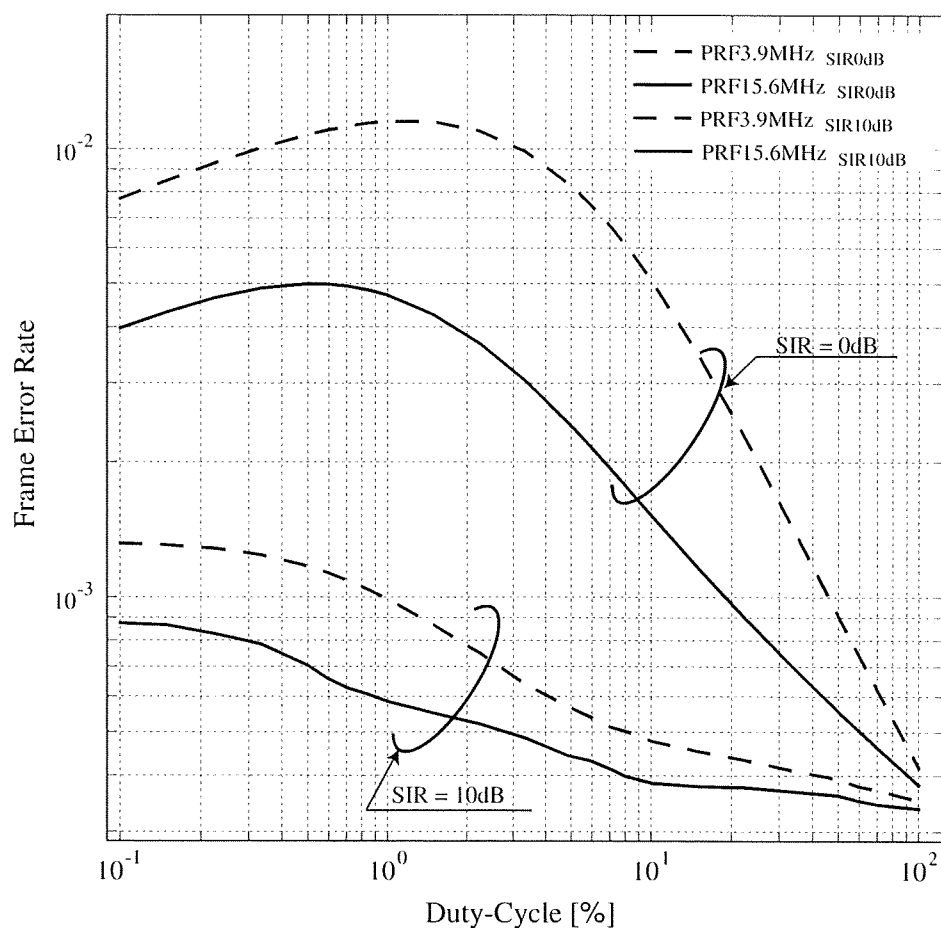


Fig. 9 The FER of the wideband OFDM system with the interference by the LDC-UWB communication devices with random polarity, when SNR = 10 dB. The definition of UWB transmission power is fixed power per unit of time

We can conclude that LDC algorithm is an efficient interference mitigation technique for low data rate UWB communication since the FER of wideband OFDM systems is improved with decreasing of the duty-cycle of LDC-UWB. However, LDC cannot suppress interference to wideband OFDM systems completely. Though, it can be mitigated moderately without additional complexity such as DAA. Thus, the duty-cycle of LDC-UWB should be chosen carefully in consideration of the quality of the service required by the wideband OFDM system in the physical layer. Moreover, the duty-cycle of LDC-UWB system should be chosen carefully in consideration of the requirements of the each LDC-UWB application.

References

1. FCC. (2002). First Report and Order: In the matter of Revision of Part 15 of the Commission's Rules Regarding Ultra-Wideband Transmission Systems. FCC 02-48, April 2002.
2. Win, M. Z., & Scholtz, R. (2000). Ultra-wide bandwidth time-hopping spread-spectrum impulse radio for wireless multiple-access communications. *IEEE Transaction on Communication*, 48(4), 679–691.
3. Freescale Semiconductor, Inc. (2005). UWB mask proposal for industry. *International Telecommunication Union Radio Communication Study Group*, document -8/429-E, October 2005.
4. Zasowski, T., & Wittneben, A. (2006). Performance of UWB systems using a temporal detect-and-avoid mechanism. In *The international conference on ultra-wideband*, September 2006.
5. Somayazulu, V. S., Foerster, J. R., & Roberts, R. D. (2006). Detect and Avoid (DAA) Mechanisms for UWB Interference Mitigation. In *The international conference on ultra-wideband*, September 2006.

6. Kogane, R., Fujii, M., Itami, M., & Itoh, K. (2006). A study on the detection scheme of the 4G signal for FSS operation in MB-OFDM. IEICE Technical Report, WBS2006-12, pp. 25–30, July 2006.
7. Yamaguchi, H. (2006). Detection-and-Avoidance (DAA) Technology for UWB—Challenges to share the frequency resource. IEICE Technical Report, WBS2005-76, pp. 11–18, March 2006.
8. Durantini, A., Giuliano, R., Mazzenga, F., & Vatalaro, F. (2006). Performance Evaluation of detect and avoid procedures for improving UWB coexistence with UMTS and WiMAX systems. In *The 2006 IEEE international conference on ultra-wideband*, pp. 501–506, September 2006.
9. Cuomo, F., Martello, C., Baicchi, A., & Capriotti, F. (2002). Radio resource sharing for ad hoc networking with UWB. *IEEE Journal on Selected Area in Communications*, 20(9), 229–239.
10. Gargin, D. J. (2004). A fast and reliable acquisition scheme for detection ultra wideband impulse radio signals in the presence of multi-path and multiple access interference. In *Ultra wideband systems 2004 joint with conference on Ultra Wideband Systems and Technologies*, pp. 106–110, May 2004.
11. Yamaguchi, H. (2004). Active interference cancellation technique for MB-OFDM Cognitive Radio. In *34th European microwave conference*.
12. Batra, A., Balakrishnan, J., Aiello, G. R., Foerster, J. R., & Dabak, A. (2004). Design of a multiband OFDM system for realistic UWB channel environments. *IEEE Transaction on Microwave Theory and Techniques*, 52(9), 2139–2147.
13. Jamieson, K., Hull, B., Miu, A., & Balakrishnan, H. (2005). Understanding the real-world performance of carrier sense. In *Proceeding of the 2005 ACM SIGCOMM workshop on Experimental approaches to wireless network design and analysis*.
14. Polastre, J., Hill, J., & Culler, D. V. (2004). Low-power media access for wireless sensor networks. In *Proceedings of the ACM sensys conference*, pp. 95–107, November 2004.
15. Nakao, Y., Watanabe, K., Sato, T., & Kohno, R. (2007). A study on coexistence of WLAN and WPAN using PAN Coordinator with array antenna. SDR Forum 2007 Technical conference and product exposition, November 2007.
16. Callaway, E. (2001). Project: IEEE P802.15 Working Group for Wireless Personal Area Networks (WPANs). doc.: IEEE 802.15-01/188r1, May 2001.
17. Ye, W., & Heidemann, J. (2005). Ultra-low duty cycle MAC with scheduled channel polling. USC/ISI Technical Report ISI-TR-604, July 2005.
18. Lovelace, W. M., & Townsend, J. K. (2003). Chip discrimination for near far power ratios in UWB networks. In *Military communications conference 2003 (MILCOM 2003)*, October 2003.
19. Lovelace, W. M., & Townsend, J. K. (2003). Adaptive rate control with chip discrimination in UWB. In *IEEE conference on ultra wideband systems and technologies 2003*, November 2003.
20. Ali, M., & Uzmi, Z. A. (2006). Medium access control with mobility-adaptive mechanisms for wireless sensor networks. *International Journal of Sensor Networks 2006*, 1(3/4), 134–142.
21. Tomoki, A., Pasya, I., & Kobayashi, T. (2003). Simulation of interference effects from MB-OFDM and DS-UWB to a QPSK digital transmission system. *International symposium on ultra wideband systems*, January 2003.
22. Peled, A., & Ruiz, A. (1980). Frequency domain data transmission using reduced computational complexity algorithms. *Proceedings of the IEEE international conference on acoustics*, Denver, pp. 964–967.
23. Fazel, K., & Kaiser, S. (2003). Multi-carrier and spread spectrum systems. England: Wiley, ISBN 0-470-84899-5.

Author Biographies



Keisuke Sodeyama was born in Nagano, Japan, in 1983. He received the B.E. degree in Department of Applied Electronics from Tokyo University of Science, Chiba, Japan in 2006. He also received the M.E. degree in Electrical and Computer Engineering from Yokohama National University, Yokohama, Japan, in 2008. He is currently working toward the Ph.D. degree in electrical and computer engineering at Yokohama National University, Yokohama, Japan. He is also Research Fellow of Japan Society for the Promotion of Science (JSPS Research Fellow) and research assistant of Venture Business Laboratory at Yokohama National University. His current research interests are ultra wideband communication, medical information communication technology, body area network and information theory. He is student member of IEEE communications society. He is also student member of IEICE and SITA, Japan.



Koji Ishibashi was born in Kofu, Yamanashi, Japan in May 1979. He received his B.E. and M.E. degree in Engineering from The University of Electro-Communications, Tokyo, Japan in 2002 and 2004 respectively. He received his Ph.D. degree in Engineering from Yokohama National University, Yokohama, Japan in 2007. From 2004 to 2007, he was a research assistant of 21st century COE program: Creation of Future Social Infrastructure Based on Information Telecommunication Technology, Yokohama National University, Yokohama, Japan. Since April 2007, he has been with the Department of Electrical and Electronic Engineering, Shizuoka University, Hamamatsu, Japan, where he is currently an Assistant Professor. His current research interests are coded modulation, differential detection, collaborative communications, and cross-layer optimization. He is a member of IEEE Communications, Information Theory, and Vehicular Technology Society. He is also a member of IEICE and SITA, Japan.



Ryuji Kohno received the B.E. and M.E. degrees in Computer Engineering from Yokohama National University (YNU) in 1979 and 1981, respectively and the Ph.D. degree in Electrical Engineering from the University of Tokyo in 1984. Since 1998 he has been a Professor in YNU. During 1984–1985 he was a Visiting Scientist in Dept. EE, University of Toronto. Since 2007, he is also a Finnish Distinguished Professor (FiDiPro) in University of Oulu, Finland. Moreover, he was also a director of SONY ATL during 1998–2002 and was a director of the UWB Tech. Inst. during 2002–2006, now Medical ICT Inst. of National Institute of Information and Communications Technology (NICT), and a principal leader of MEXT 21st century COE program on Creation of Future Social Infrastructure Based on ICT during 2002–2007 and is currently a principal leader of MEXT Global COE program on Innovative Integration between Medicine and Engineering Based on ICT, during 2008–2013 as well as a director of Medical ICT Center in YNU. Prof. Kohno was

elected to be a BoG member of the IEEE Information Theory Society three times on 2000, 2002, and 2006. He was an editor of the IEEE Trans. Information Theory during 1995–1998, currently is that of the IEEE Trans. Communications since 1994 and that of the IEEE Trans. Intelligent Transport Systems since 2000. He is a fellow of IEICE (Institute of Electronics, Information, Communications Engineers), and was a Vice-President of Engineering Sciences Society of IEICE. Currently he is an Editor-in chief of the IEICE Trans. Fundamentals and also the Vice-President of SITA (Society of Information Theory and its Applications). He has contributed for organizing many international conferences, such as a TPC co-chair of the IEEE ISSSTA'92, PIMRC'93, Information Theory Workshop (ITW'93), PIMRC'99, IWUWBS'03, and a general chair of IEEE ISIT'03, UWBST & IWUWB'04, IWUWBST'05, ISMICT'06 and '07 and so on. He was awarded IEICE Greatest Contribution Award and NTT DoCoMo Mobile Science Award in 1999 and 2002, respectively.

PAPER

Hybrid ARQ Error-Controlling Scheme for Robust and Efficient Transmission of UWB Body Area Networks

Haruka SUZUKI[†], *Student Member*, Marco HERNANDEZ^{††}, *Nonmember*,
and Ryuji KOHNO^{†††}, *Fellow*

SUMMARY This paper presents hybrid type-II automatic repeat request (H-ARQ) for wireless wearable body area networks (BANs) based on ultra wideband (UWB) technology. The proposed model is based on three schemes, namely, high rate optimized rate compatible punctured convolutional codes (HRO-RCPC), Reed Solomon (RS) invertible codes and their concatenation. Forward error correction (FEC) coding is combined with simple cyclic redundancy check (CRC) error detection. The performance is investigated for two channels: CM3 (on-body to on-body) and CM4 (on-body to a gateway) scenarios of the IEEE802.15.6 BAN channel models for BANs. It is shown that the improvement in performance in terms of throughput and error protection robustness is very significant. Thus, the proposed H-ARQ schemes can be employed and optimized to suit medical and non-medical applications. In particular we propose the use of FEC coding for non-medical applications as those require less stringent quality of service (QoS), while the incremental redundancy and ARQ configuration is utilized only for medical applications. Thus, higher QoS is guaranteed for medical applications of BANs while allowing coexistence with non-medical applications.

key words: *Type-II Hybrid ARQ, Body Area Network(BAN), Rate Compatible Punctured Convolutional Code (RCPC), Reed Solomon (RS) Invertible Codes, IEEE802.15.6, Ultra Wide Band(UWB)*

1. Introduction

Body area networks (BANs) have emerged as an important subject in personal wireless communications, recently. Indeed, the standardization task group IEEE 802.15.6 pursues the standardization of PHY and MAC layers for BANs nowadays. The potential mass market includes medical and non-medical applications. As they require different quality of service (QoS) in terms of reliability and performance, a fixed error control mechanism like forward error correction (FEC) is not appropriate. Most cases of non-medical applications do not require strong error control but less complexity and power consumption, and in the special case of video transmission a large throughput and low latency are needed.

Manuscript received August 28, 2009.

[†]The author is with the Division of Physics, Electrical and Computer Engineering, Yokohama National University(YNU), Yokohama-city, 240-8501 JAPAN.

^{††}The author is with Medical ICT Group, National Institute of Information and Communications Technology(NICT), Yokosuka-city, 239-0847 JAPAN.

^{†††}The author is with YNU and NICT, JAPAN.

DOI: 10.1587/transcom.E0.B.1

On the contrary, medical applications require high reliability and relative low data rate transmission as well high data rate transmission. Hence, strong error control is expected while relatively larger complexity is allowed. Thus, in order to reconcile between medical and non-medical applications requirements, we propose an adaptive error control mechanism in the form of hybrid type II ARQ (H-ARQ). Such error system adapts to the channel conditions which can optimize the throughput, latency and reliability according to the application specification and channel conditions.

The proposed scheme can be used for both narrowband and wideband PHYs. Although, in the current status of the task group IEEE 802.15.6, non-medical applications are envisioned for the wideband PHY proposal only, i.e., UWB-PHY. On the other hand, medical applications use the narrowband and wideband PHYs [1]. Therefore, we focus on the UWB-PHY for designing and showing the coexistence of medical and non-medical applications for BANs through the proposed HARQ.

UWB systems have emerged as a potential candidate for on-body communications in BANs [1]. Practical implementations of UWB systems for BANs with current technology are non-coherent architectures. Indeed, BAN devices require very low power consumption due to constraint imposed by battery's power and lifespan. In contrast, coherent transceivers in the UWB regime demand high power consumption. Therefore, we propose a simple and practical 2PPM modulation scheme with energy detection at the receiver. This makes it feasible to implement and analog front-end at the receiver (with low power consumption) in the high band of UWB, where UWB-BANs are proposed to operate, globally. In this paper, it is assumed that interference among coexisting piconets BANs, because a coordinator in each piconet BAN of IEEE802.15.6 can control access of all the devices within its coordinating piconet so as to avoid contention among accesses of all the devices although interference among coexisting piconet BANs due to asynchronous access among the coexisting piconets. Since high band of UWB regulation such as 7.25-10.25GHz has suppressed interference enough low to coexisting other radios. However, non-coherent transceivers have poorer performance than coherent architectures. Therefore, it is necessary to in-

roduce an error control mechanism that can guarantee QoS and performance depending on the application and channel condition, while relying in a simple UWB-PHY.

We study three forms of HARQ for BANs, namely, hybrid type II ARQ based on rate compatible punctured convolutional codes (RCPC), half-rate invertible coding and concatenated coding. The rest of the paper is divided as follows: Section II delineates the system and the signal. Section III illustrates hybrid type II ARQ proposal, which is based on RCPC and invertible codes, Section IV shows simulation results and evaluates their performances. Such simulation results are presented for the scenarios CM3 (on-body to on-body devices) and CM4 (on-body to a gateway)[1]. Finally, Section V conclusions are drawn.

2. System and Signal Model of Wireless Body Area Network

2.1 System Model

Medical and non-medical applications need to coexist in BANs. As the network topology is star, the communication links are performed between on-body or in-body devices and a single central controller or coordinator. In particular, the communication link for medical applications require higher reliability or QoS in contrast to non-medical applications as shown Table 1. Consequently, it increasing QoS means to increase complexity and power consumption.

Table 1 QoS Requirement

Category	Medical	Non-medical
Main usage	Data storage	Fitness/Games (Real-time)
Bit error rate	$\leq 10^{-6}$	$\leq 10^{-3}$
Data rate	100kbps – 10Mbps	1 – 10Mbps
Key requirement	Reliability	Latency

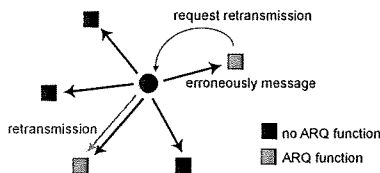


Fig. 1 The formation of the star topology for Wireless BANs

As HARQ combines FEC and retransmission, the main purpose is to design the FEC such that it corrects the error patterns that appear frequently in the channel. The FEC is maintained with low complexity as much as possible. On the other hand, when error patterns that appear less frequently like time-varying behavior and/or deep fades, a retransmission is requested.

Hence, a fine balance between throughput and error correction is achieved, which makes the system is more reliable.

This is only required for high QoS medical applications. Hence, in order to harmonize medical a non-medical applications, we propose that non-medical devices employ only FEC and medical devices are HARQ enable, i.e., incremental redundancy and retransmissions are allowed. The maximum number of retransmissions is bounded to end-to-end delay or latency of the system. Currently, such latency parameter is under study in the IEEE 802.15.6 TG.

2.2 Signal Model

The paper assumes non-coherent modulation in the form of PPM and energy detection. This is the most promising candidate as mandatory mode for the wide-band PHY of the IEEE 802.15.6 TG on BANs.

Hence, the transmitting UWB signal is given by

$$x(t) = \sum_m w(t - g_m T_{BPM} - m T_{sym}), \quad (1)$$

$$w(t) = \sum_{n=0}^{N_{cpb}-1} d_{m,n} p(t - nT_c), \quad (2)$$

where $g_m \in \{0, 1\}$ is the m th component of a given codeword, T_{BPM} is the slot time for 2PPM, and T_{sym} is the symbol time. The basis function $w(t)$ is a burst of short pulses $p(t)$, where $d_{m,n}$ is a scrambling sequence and N_{cpb} is a sequence length. This is only to control data rate and legacy to IEEE 802.15.4a systems.

For the sake of illustration and without losing generality, it is assumed that $N_{cpb} = 1$ and $d_{m,0} = 1 \forall m$. Moreover, $p(t)$ is a modulated square root raised cosine (SRRC) pulse waveform with duration $T_p = 2$ nsec, roll-off factor of 0.5 and truncated to 8 pulse times. The central frequency f_c is 7.9872 GHz (corresponding to the 9th band of the IEEE 802.15.4a band plan) and the bandwidth is 499.2 MHz.

3. Type II Hybrid ARQ Scheme for BANs

3.1 Proposed System Configuration

As mentioned above, the proposed system is HARQ type II. In such scheme, only parity bits are sent some retransmissions. Erroneous packets are not discarded and the decoder can employ previously received packets. The main characteristics are requires low coding overhead and is suitable for bursty (time-varying) channels.

Figures 2 and 3 show the flow chart and the system model of the proposed system, respectively. In our proposed system, both of the medical and non-medical

applications use the same modulation and demodulation schemes. But only the medical application has a H-ARQ function. Hence, when the lack of the reliability has detected, the medical devices can request a retransmission.

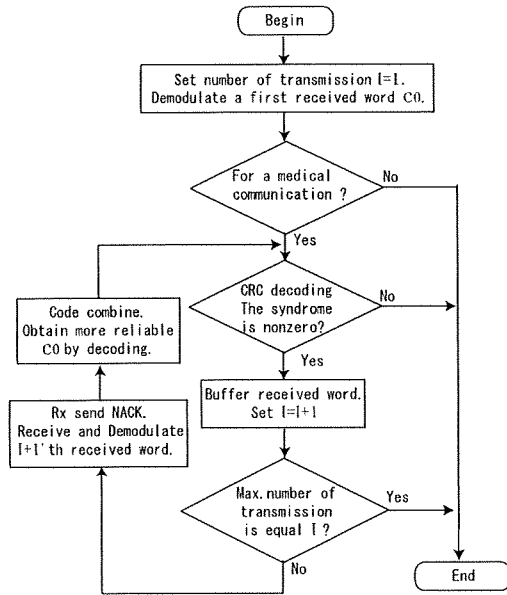


Fig. 2 The flow chart of the proposed system

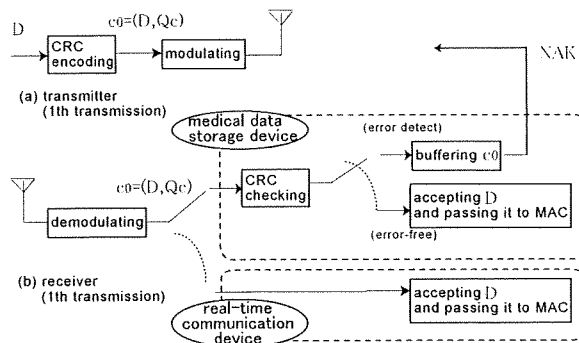


Fig. 3 The flow chart of the proposed system

The HARQ type II requires two types of coding, namely, a high rate error detection cyclic redundancy check (CRC) codes C_c , $Q_c = C_c(D)$, where Q_c is CRC parity bits of data D . And FEC C_i for error correction, $Q_i = C_i(D)$, where Q_i is FEC parity bits of data D .

3.2 Generic HARQ Type II

In section 3.2, we describe the generic H-ARQ Type II.

3.2.1 HARQ Type II Generic Flow Algorithm

1 : Tx sends $c_0 = (D, Q_c)$

if Rx determines message is error free using C_c then
 Rx accepts message and passes it to the MAC
 else
 Rx sends a NACK
 end if
 2 : Tx sends parity bits.
 if Rx determines message is error free using C_c and C_i then
 Rx accepts message and passes it to the MAC
 else
 Rx sends a NACK
 go to 1) or 2) (depending on the HARQ strategy)
 end if

3.2.2 Rate Compatible Punctured Convolutional Code

The reason of studying the rate compatible punctured convolutional codes (RCPC) is because it has the strong error correcting capabilities [2]. Moreover, non-medical cases can obtain moderate code rates.

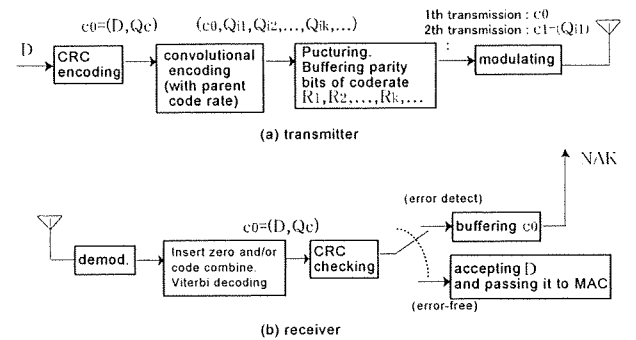


Fig. 4 Generic system model of Hybrid ARQ protocol using HRO-RCPC codes

First, a message D is encoded with C_c as written by $c_0 = (D, Q_c)$, where Q_c is CRC parity bits and c_0 is the first transmission codeword that we obtain. Let \hat{c}_0 denotes a received first codeword. The receiver computes the syndrome of $\hat{c}_0 = (\hat{D}, \hat{Q}_c)$ based on C_c . If the syndrome is zero, \hat{D} is error-free and consequently, a *ACK* is sent to the transmitter. On the other hand, if the syndrome is nonzero, the presence of errors in \hat{D} is detected. The erroneous codeword \hat{c}_0 is then saved in the receiver and a *NAK* is sent to the transmitter. After receiving this *NAK*, the transmitter sends $c_1 = (Q_{i1})$, which is RCPC parity bits of code rate R_1 .

In this scheme, the transmission starts with the code of the highest rate. If the code word is received with error, a retransmission is requested and the transmitter sends the next code incrementally with lower rate. Thus, code rates, R_k , are given in decreasing

order $R_k > R_{k+1}$, where k represents the k th transmission. This codeword is combined at the receiver with previously erroneously received incremental codewords. Then it is decoded and checked for a detectable error. This procedure repeats until error free reception is achieved.

3.2.3 Invertible Codes

In a RCPC-based HARQ, a Viterbi decoding is required. If the constraint length is high, the complexity is a concern. Moreover, when the parent code rate is very low, the buffer size is also a problem. Thus, we employ the systematic and invertible RS codes with the code rate about $1/2$ as FEC [6]. So, decoding complexity is reduced.

The second type of hybrid type-II ARQ protocol is based on invertible codes. A code is said to be invertible when knowing only the k' parity-check bits of a codeword, the corresponding $k (\leq k')$ information bits can be uniquely determined by an inversion process [?,]. BCH codes and RS codes are the examples of this invertible codes.

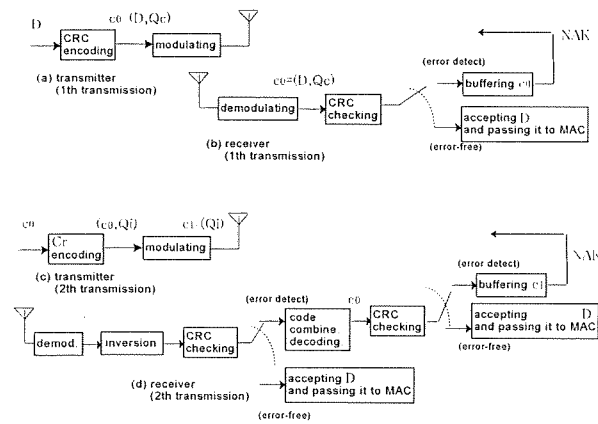


Fig. 5 Generic system model of Hybrid ARQ protocol using invertible codes

Figure 5 shows the system of the invertible code protocol. Two linear codes are also used in this scheme: one is a code C_c , which is designed for error detection, and the other one is an invertible code C_i , which is designed for error correction.

First, the codeword $c_0 = (D, Q_c)$ is transmitted. After receiving a NAK, the transmitter computes the parity bits Q_i , which is encoded with C_i they written by (c_0, Q_i) . Then we obtain a second transmission codeword $c_1 = (Q_i)$. Once c_1 is received, the receiver processes inversion, after computes the syndrome. If the syndrome is nonzero, the receiver processes code combine with buffering codeword c_1 , and decodes for error correction based on the code C_i . Otherwise, if the syndrome is zero, the receiver computes inversion

and accepts D . Upon receiving the second NAK for the message D , the transmitter re-sends the codeword $c_0 = (D, Q_c)$ and the process is repeated. Therefore, the retransmissions are alternate repetitions of the information codeword $c_0 = (D, Q_c)$ and the parity codeword $c_1 = (Q_i)$. The receiver stores either the received c_0 or parity block c_1 alternatively. The retransmissions continue until the message D is finally recovered either by inversion or decoding process.

3.3 Proposed system using Concatenated Coding

In section 3.3, we describe the proposed H-ARQ Type II. The idea is to start with RS-based HARQ for the first transmission (information bits) and first retransmission (parity bits). So the non-medical devices is not needed to have the function of decoding. It is different from the generic H-ARQ in satellite communications and so on.

3.3.1 Concatenation of RS and RCPC codes

In order to improve performance, we propose to use concatenated coding with $RS(n, k)$ as outer codes and RCPC as inner codes. If the algorithm determines that the error pattern cannot be corrected, then information bits and RS parity bits are concatenated with RCPC coding. Consequently, if errors cannot be corrected in this fashion, incremental redundancy is applied.

Figure 6 shows the flow of the proposed scheme.

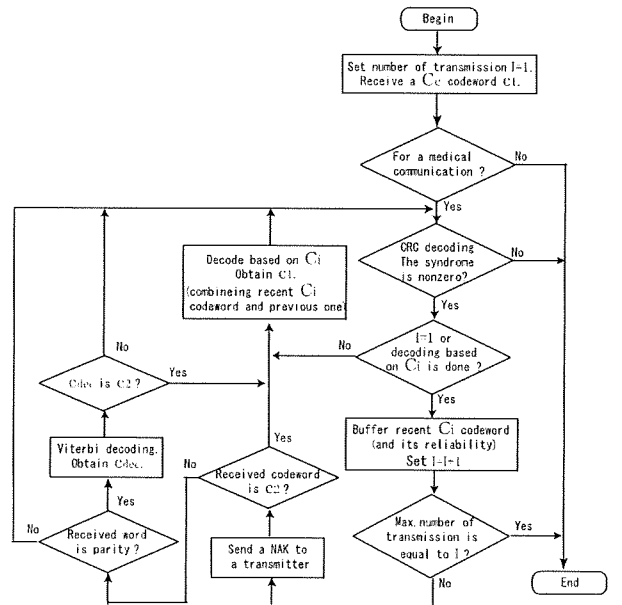


Fig. 6 The flow chart of the proposed concatenated coding.

First, a message D is encoded with C_c that written by $c_0 = (D, Q_c)$, where Q_c is CRC parity bits